# Transverse momentum fluctuations – system size dependence (status of the draft)

Katarzyna Perl
Institute of Experimental Physics
Warsaw University

# Plan of the draft

1. Introduction
2. Measures of fluctuations
3. Experimental Set-up
4. Data selection and analysis
   - 4.1 Data sets
   - 4.2 Event and particle selection
   - 4.3 Corrections and systematic error estimates
5. Results
6. **Discussion**
7. **Summary**

# 1. Introduction

- The main goals of event-by-event physics
- Dynamical fluctuations
- The subject of this paper – system size dependence of transverse momentum fluctuations

# 2. Measures of fluctuations

- Distribution of mean (per event) transverse momenta $M(p_T)$ for data and mixed events
- $\phi_{pT}$ correlation measure
- Two-particle correlation plots $(x_1,x_2)$

# 3. Experimental Set-up

- TPCs
- Different beam definitions (counters) and target arrangements (p+p, C+C, Si+Si and Pb+Pb)
- VCAL

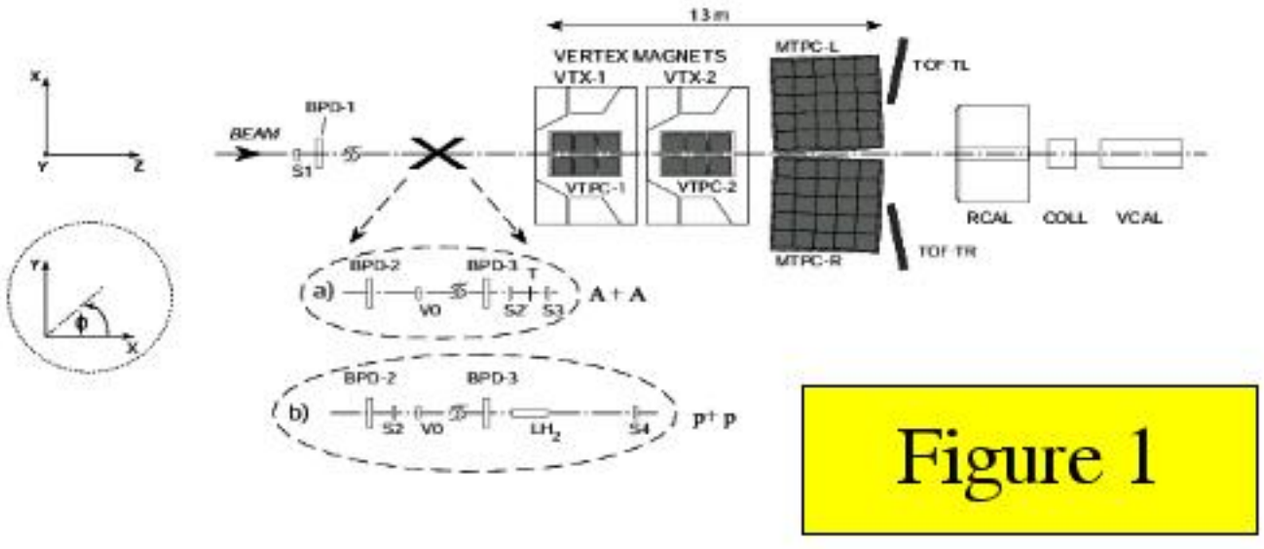


Figure 1: The experimental set-up of the NA49 experiment [21] with different beam

Figure 1

# 4. Data selection and analysis

- 4.1 Data sets

| | No. of events | $\sigma/\sigma_{tot}$ | $\langle N_W \rangle$ | $b$ range $[fm]$ |
|---|---|---|---|---|
| p+p | 570 000 | 0.9 | 2 | |
| C+C | 33 000 | 0.153 | 13.9 | 0 - 2.0 |
| Si+Si | 63 000 | 0.122 | 37 | 0 - 2.6 |
| Pb+Pb(6) | 117 000 | 0.57 | 42 | 10.2 - |
| Pb+Pb(5) | 59 000 | 0.10 | 88 | 9.1 - 10.2 |
| Pb+Pb(4) | 68 000 | 0.10 | 134 | 7.4 - 9.1 |
| Pb+Pb(3) | 68 000 | 0.11 | 204 | 5.4 - 7.4 |
| Pb+Pb(2) | 45 000 | 0.075 | 281 | 3.4 - 5.4 |
| Pb+Pb(1) | 180 000 | 0.05 | 352 | 0 - 3.4 |

Table 1: Data sets used in analysis. Listed for p+p, C+C, Si+Si and six centralities of Pb+Pb collisions at 158 $A$GeV are: number of events, $\sigma/\sigma_{tot}$ - the fraction of the total inelastic cross section, $\langle N_W \rangle$ - the mean number of wounded nucleons, $b$ - impact parameter.

| $y_\pi$ | $A[\frac{c}{GeV}]$ | $B[\frac{GeV}{c}]$ | $C[\frac{deg.^2 GeV}{c}]$ |
|---|---|---|---|
| 3.9 - 4.1 | 0 | 0.3 | 6500 |

Table 1

# 4.2 Event and particle selection

* vertex cuts
* track cuts (bx, by, nmp, np/nmp)
* $4.0 < y_{\pi} < 5.5$
* $0.005 < p_T < 1.5$ GeV/c
* geometrical acceptance ( $p_T$ versus azimuthal angle)

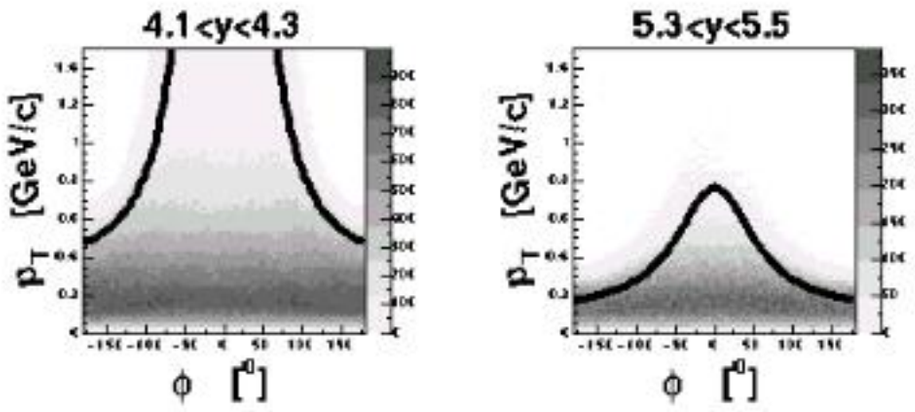


Figure 2

Table 2

Pb+Pb collisions at 158 $A$GeV are: number of events, $\sigma/\sigma_{tot}$ - the fraction of al inelastic cross section, $\langle N_W \rangle$ - the mean number of wounded nucleons, $b$ - imp ameter.

| $y_\pi$ | $A[\frac{c}{GeV}]$ | $B[\frac{GeV}{c}]$ | $C[\frac{fm^3 GeV}{c}]$ |
|---|---|---|---|
| 3.9 - 4.1 | 0 | 0.3 | 6500 |
| 4.1 - 4.3 | 0 | 0.3 | 5500 |
| 4.3 - 4.5 | 0 | 0.25 | 4500 |
| 4.5 - 4.7 | 0 | 0.25 | 3500 |
| 4.7 - 4.9 | 0 | 0.2 | 2500 |
| 4.9 - 5.1 | 0.5 | 0.2 | 2500 |
| 5.1 - 5.3 | 1.0 | 0.1 | 2500 |
| 5.3 - 5.5 | 1.5 | 0.1 | 2500 |

ble 2: The parametrization of NA49 $y - p_T$ acceptance at 158 $A$GeV for positiv rged particles (STD+). For negatively charged particles one has to redefine azimut gle and use the same parametrization.

# 4.3 Corrections and systematic error estimates

* influence of non-target interactions
* influence of non-vertex tracks

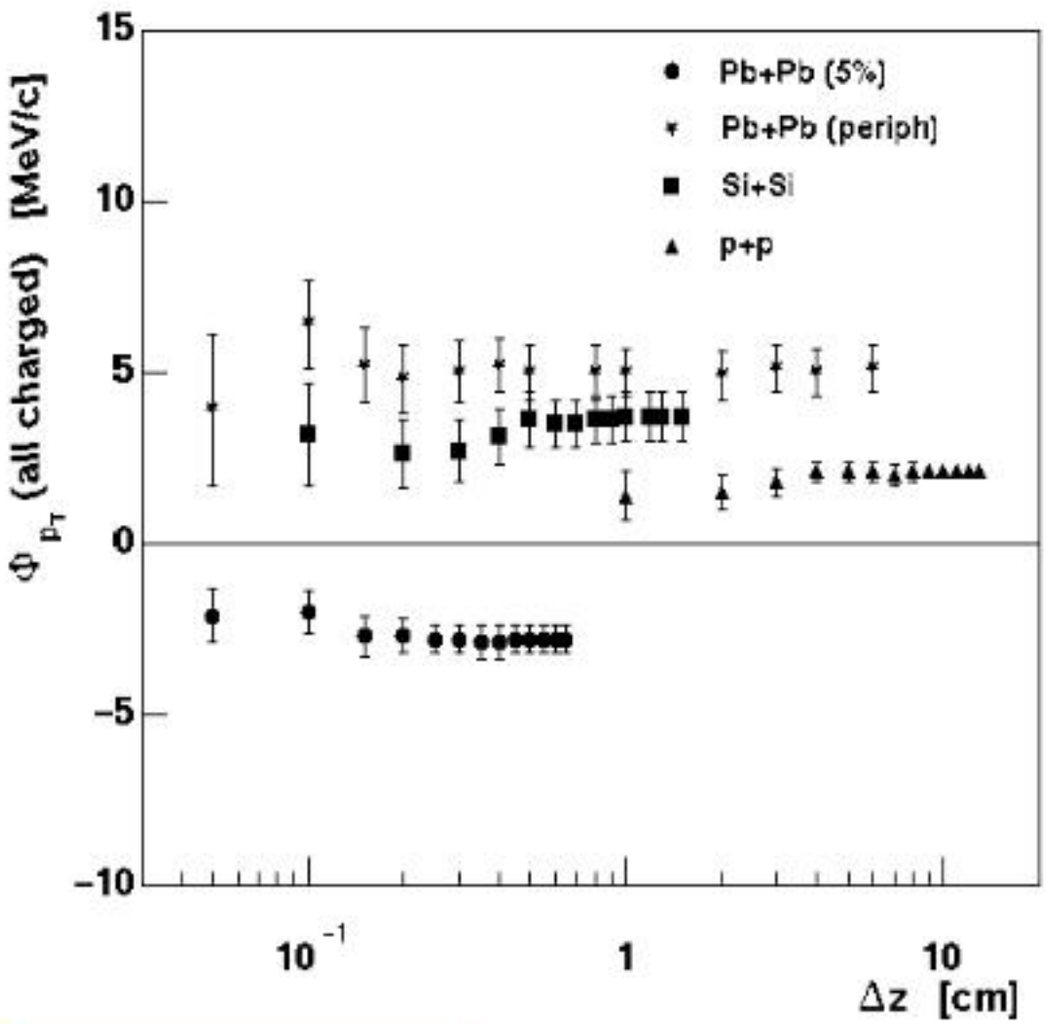


Figure 3

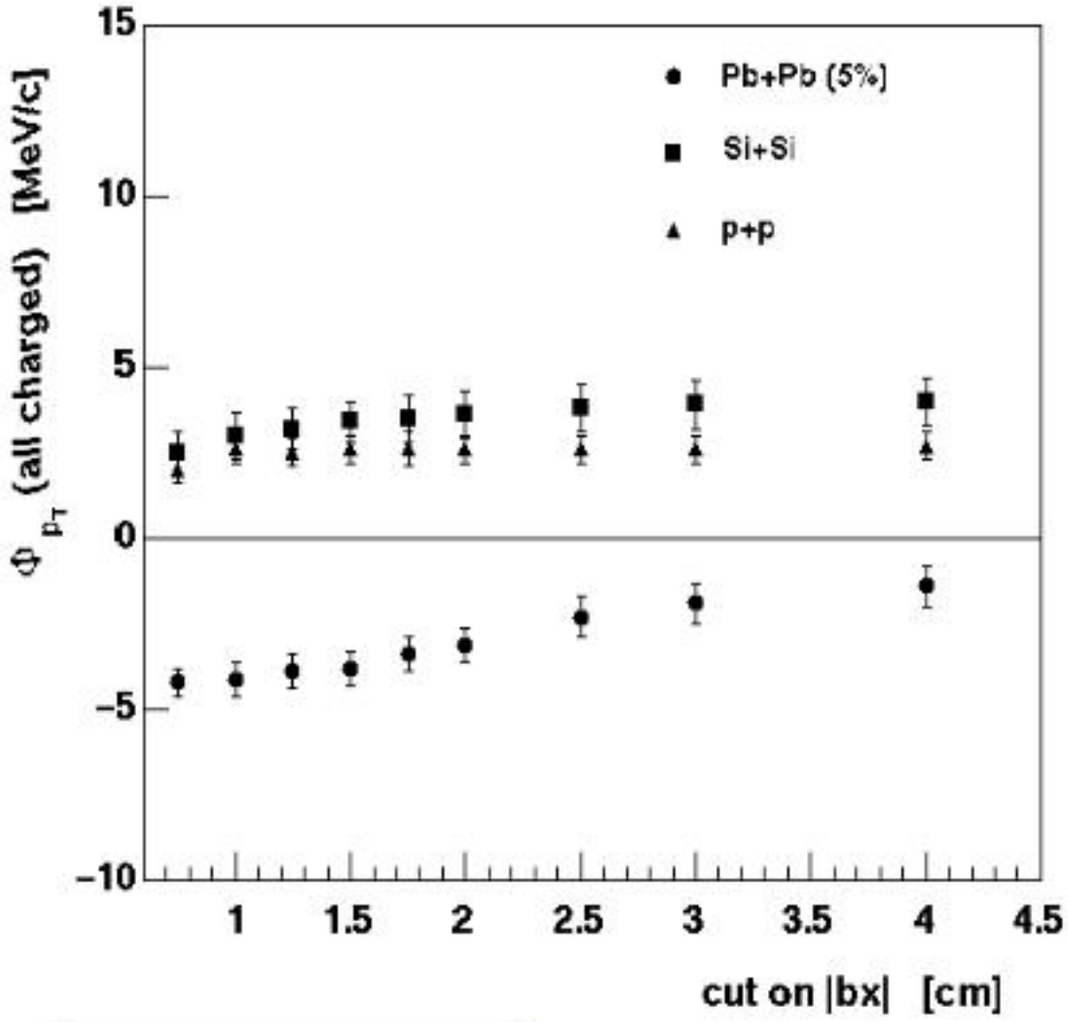


Figure 4

# 4.3 Corrections and systematic error estimates

* losses of tracks due to reconstruction inefficiency and track selection cuts
* limited two track resolution effect

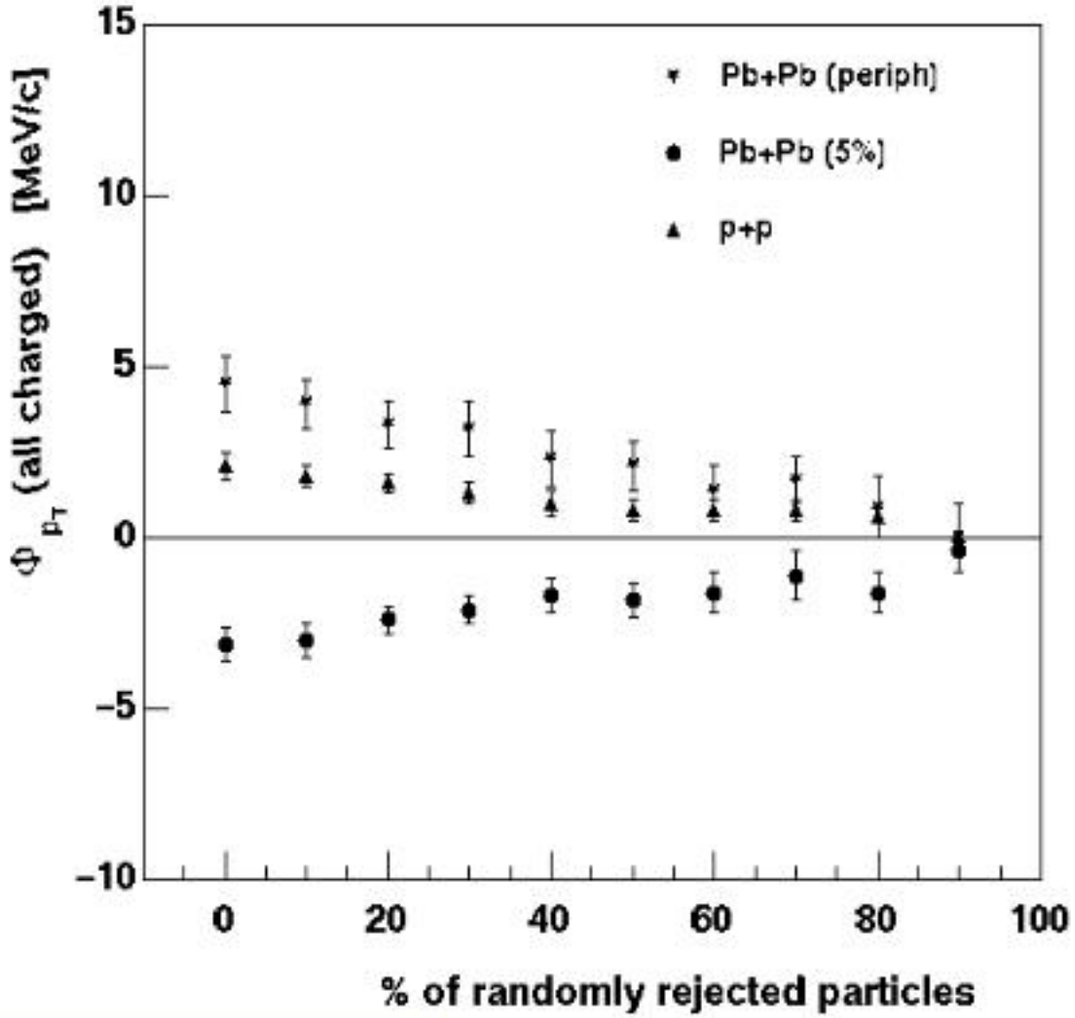


Figure 5

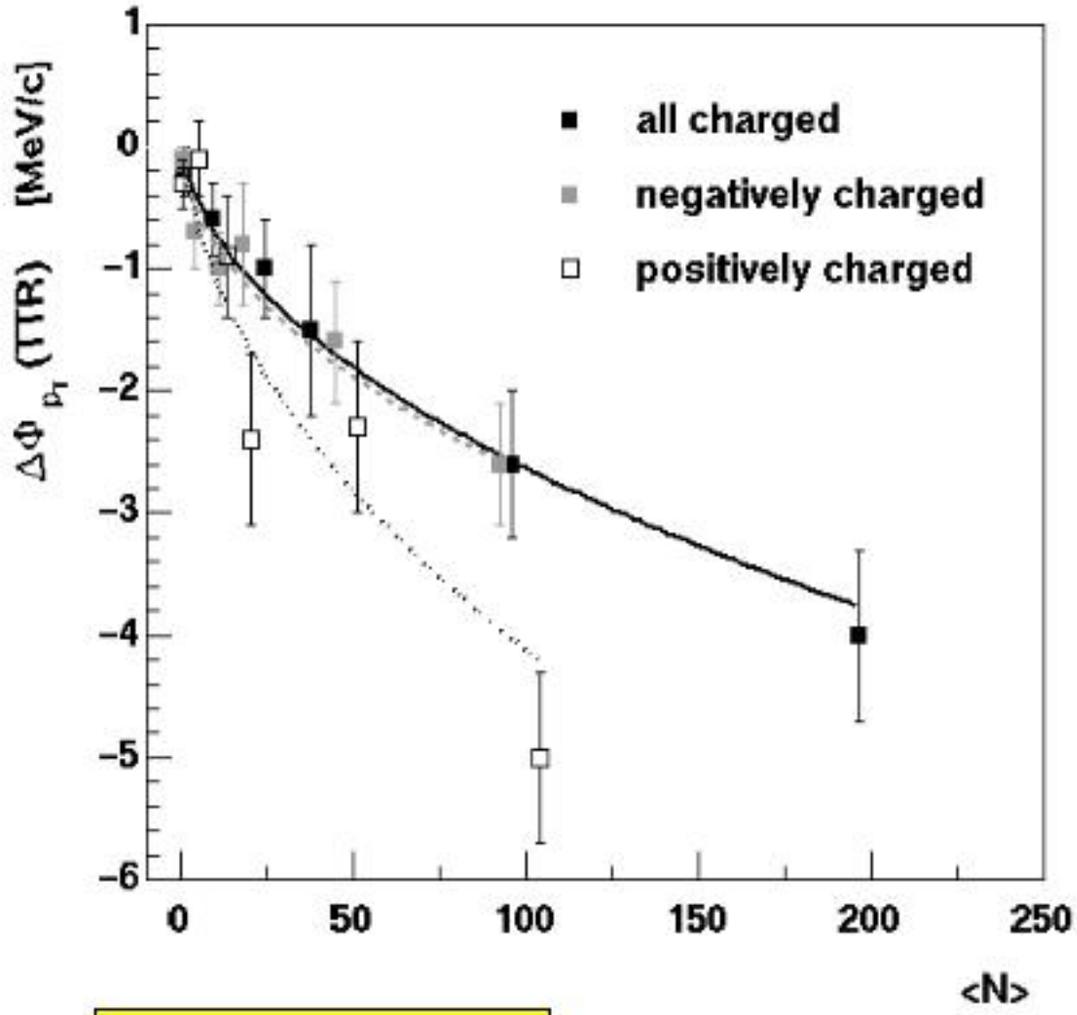


Figure 6

# 5. Results

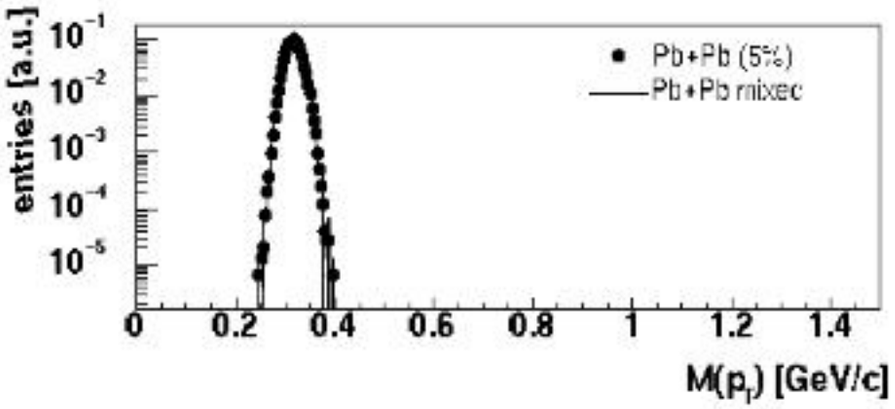


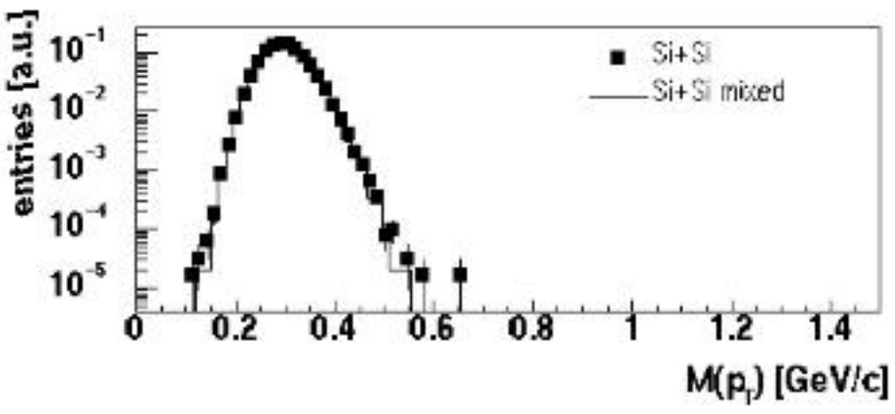


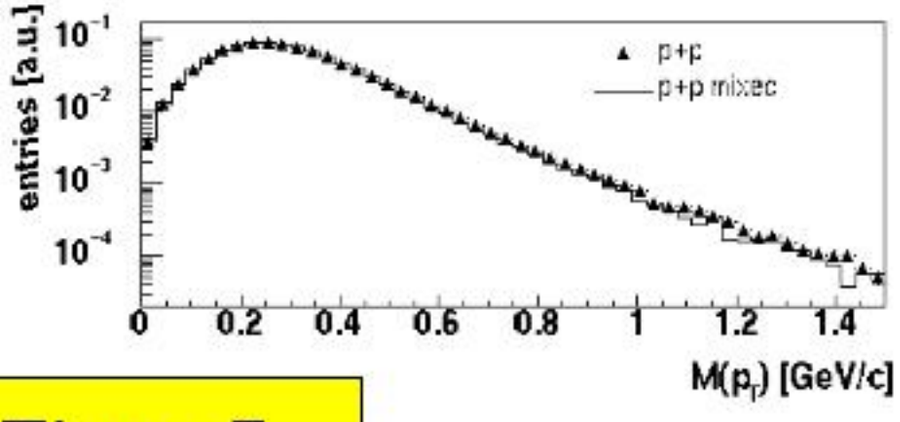


Figure 7

| | $\langle N \rangle$ | $\sigma(N)$ | $\overline{p_T}$ [MeV/c] | $\sigma(p_T)$ [MeV/c] | $\Phi_{p_T}$ [MeV/c] |
|---|---|---|---|---|---|
| p+p (all) | 1.4 | 1.3 | 304 | 196 | 2.2 ± 0.3 |
| p+p (-) | 0.6 | 0.7 | 283 | 179 | 0.8 ± 0.1 |
| p+p (+) | 0.8 | 0.9 | 317 | 206 | -1.4 ± 0.3 |
| C+C (all) | 10 | 4.3 | 300 | 210 | 5.4 ± 0.7 |
| C+C (-) | 4.5 | 2.4 | 279 | 190 | 1.8 ± 0.8 |
| C+C (+) | 5.5 | 2.7 | 317 | 224 | 0.7 ± 0.7 |
| Si+Si (all) | 27 | 7 | 301 | 217 | 4.9 ± 0.8 |
| Si+Si (-) | 12 | 4 | 277 | 195 | 2.6 ± 0.5 |
| Si+Si (+) | 15 | 4 | 320 | 231 | -0.2 ± 0.7 |
| Pb+Pb(6) (all) | 39 | 18 | 299 | 220 | 7.2 ± 0.7 |
| Pb+Pb(6) (-) | 18 | 9 | 270 | 195 | 4.5 ± 0.5 |
| Pb+Pb(6) (+) | 21 | 10 | 325 | 237 | 1.9 ± 0.7 |
| Pb+Pb(5) (all) | 73 | 17 | 305 | 226 | 6.6 ± 0.7 |
| Pb+Pb(5) (-) | 34 | 9 | 273 | 199 | 4.5 ± 0.7 |
| Pb+Pb(5) (+) | 39 | 9 | 333 | 245 | 0.6 ± 0.8 |
| Pb+Pb(4) (all) | 104 | 19 | 309 | 230 | 5.6 ± 0.8 |
| Pb+Pb(4) (-) | 49 | 10 | 276 | 202 | 3.8 ± 0.5 |
| Pb+Pb(4) (+) | 55 | 11 | 337 | 249 | -0.6 ± 0.9 |
| Pb+Pb(3) (all) | 148 | 21 | 312 | 233 | 4.6 ± 0.8 |
| Pb+Pb(3) (-) | 69 | 11 | 279 | 204 | 2.9 ± 0.8 |
| Pb+Pb(3) (+) | 79 | 12 | 342 | 252 | -1.3 ± 0.8 |
| Pb+Pb(2) (all) | 193 | 21 | 315 | 234 | 2.2 ± 1.0 |
| Pb+Pb(2) (-) | 90 | 11 | 281 | 205 | 2.4 ± 0.8 |
| Pb+Pb(2) (+) | 103 | 13 | 344 | 254 | -3.7 ± 1.1 |
| Pb+Pb(1) (all) | 230 | 19 | 317 | 236 | 1.4 ± 0.8 |
| Pb+Pb(1) (-) | 108 | 11 | 281 | 203 | 0.9 ± 0.6 |
| Pb+Pb(1) (+) | 122 | 12 | 349 | 257 | -2.9 ± 0.8 |

Table 3: Measured inclusive and event-by-event parameters for accepted particles. $\langle N \rangle$, $\sigma(N)$, $\overline{p_T}$ and $\sigma(p_T)$ values are not corrected for acceptance. $\Phi_{p_T}$ values are corrected for limited two track resolution. The systematic error of $\Phi_{p_T}$ is smaller than 1.6 MeV/c.

Table 3

# 5. Results

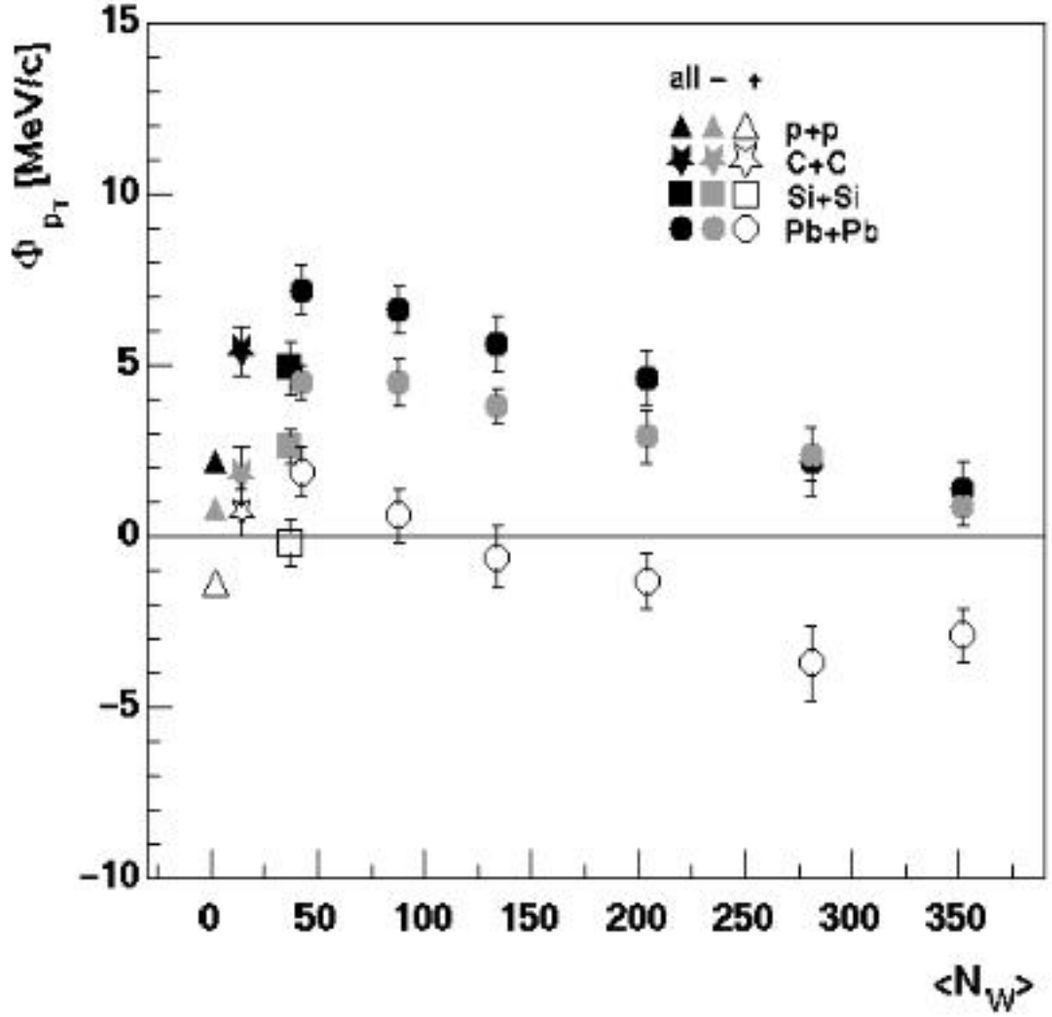


Figure 8

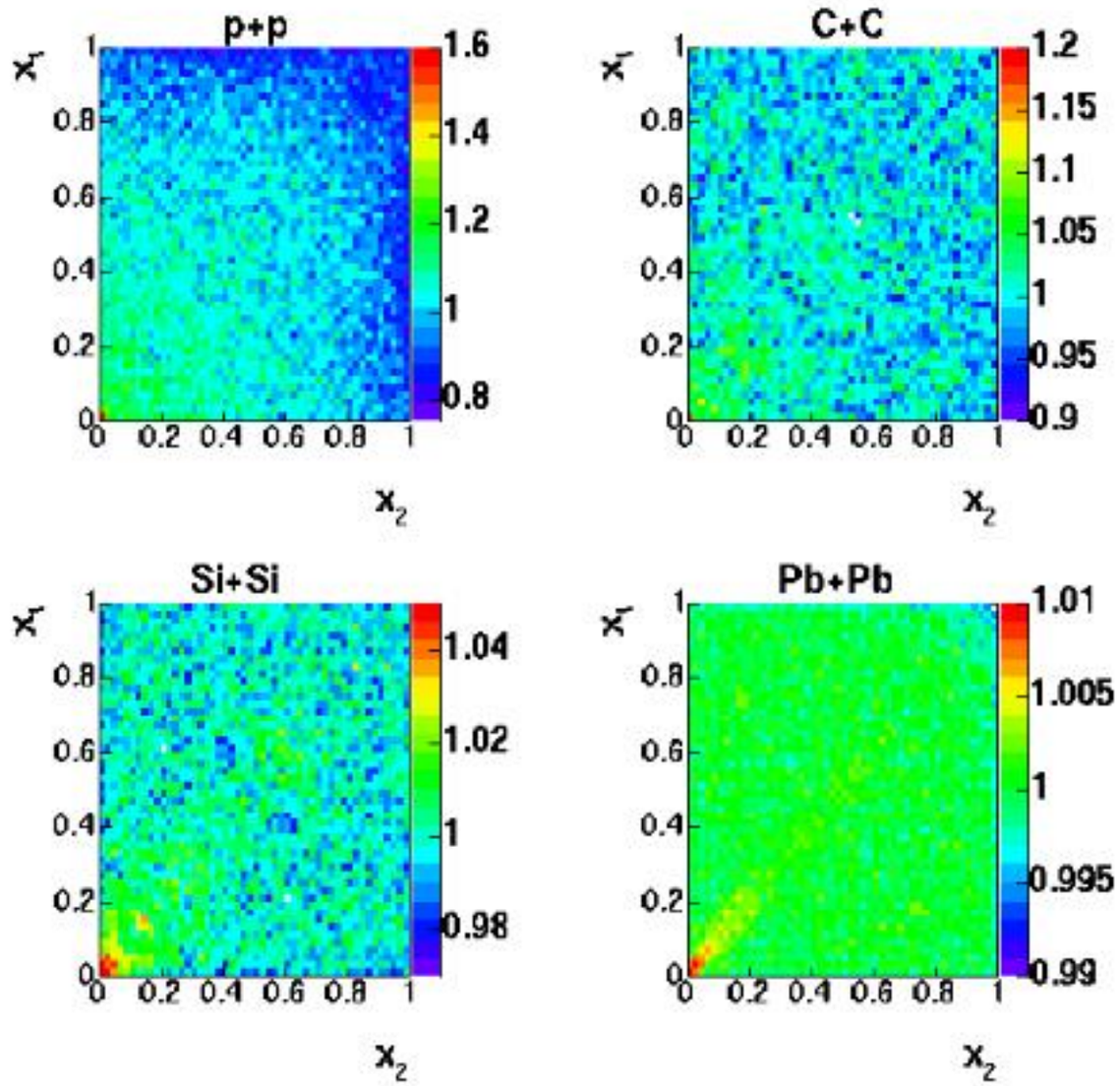


Figure 9

# 6. Discussion

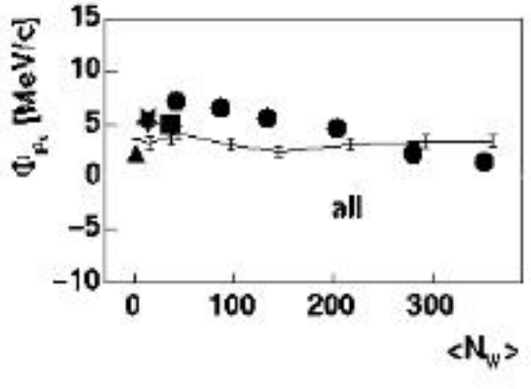


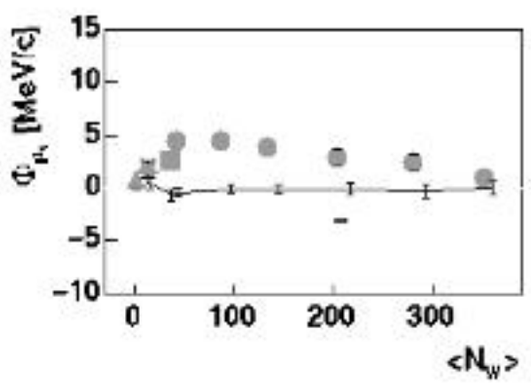


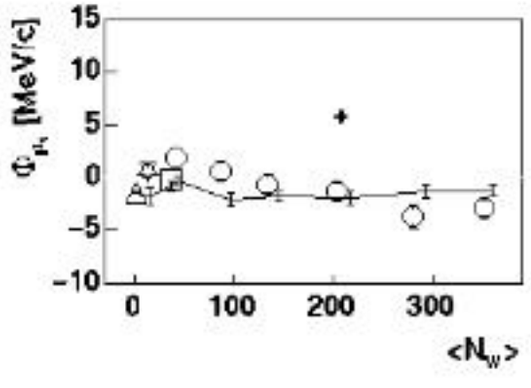


- HIJING model with NA49 acceptance and kinematical cuts
- No significant centrality dependence

Figure 10

# 6. Discussion

- Low $\Phi_{pT}$ values for p+p (data and HIJING)
- Structure for two-particle correlation plot (p+p) -> what is the origin ?

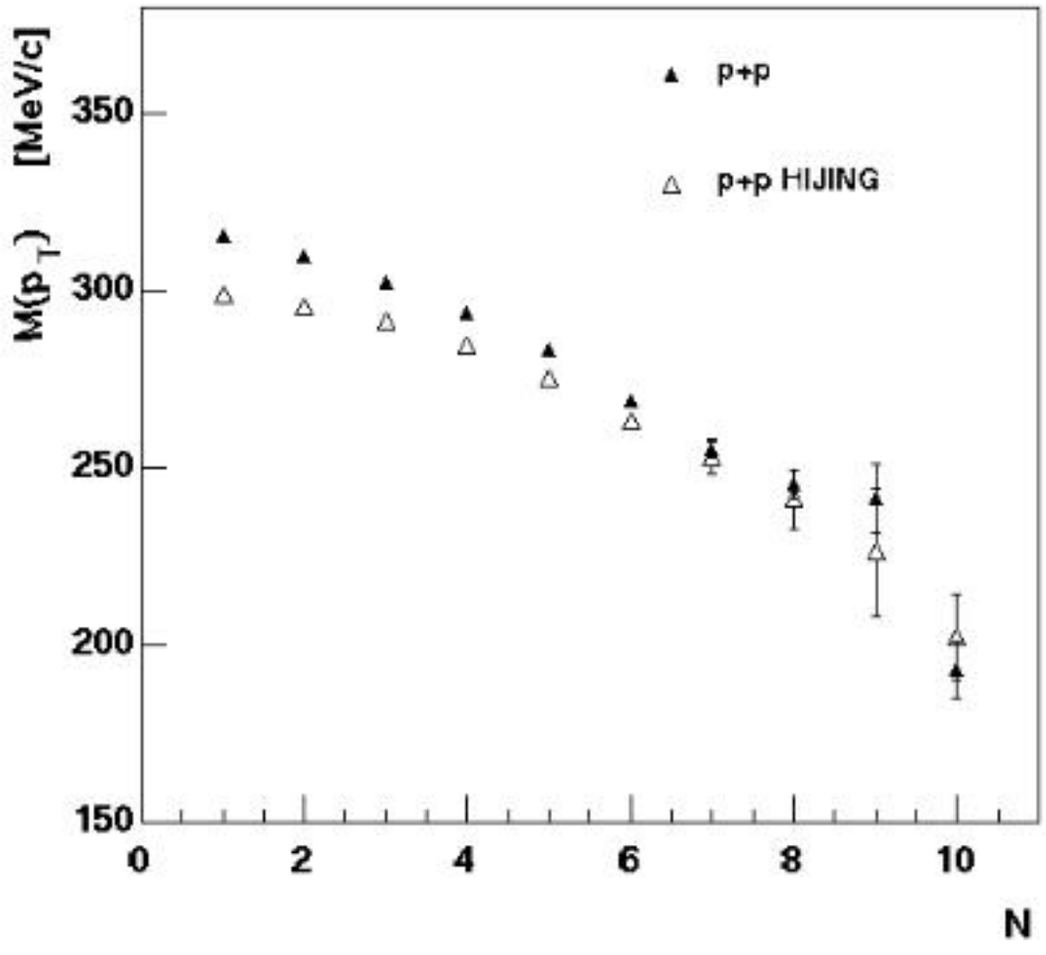


Figure 11

# 6. Discussion

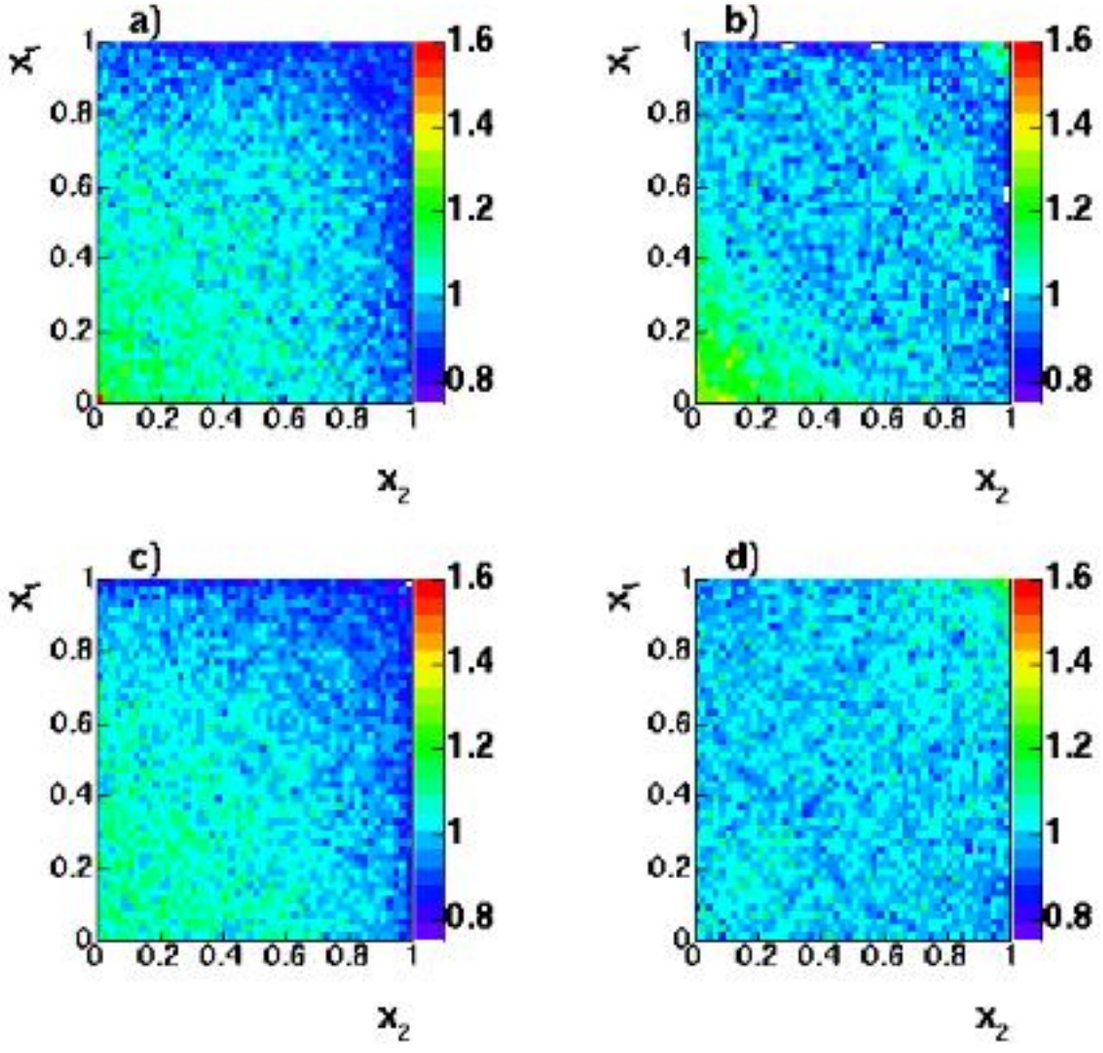


Figure 12

- a) p+p data
- b) HIJING model
- c) random generator with $M(p_T)$ versus N dependence
- d) fluctuation of the inverse slope parameter (10.5%)

# 6. Discussion

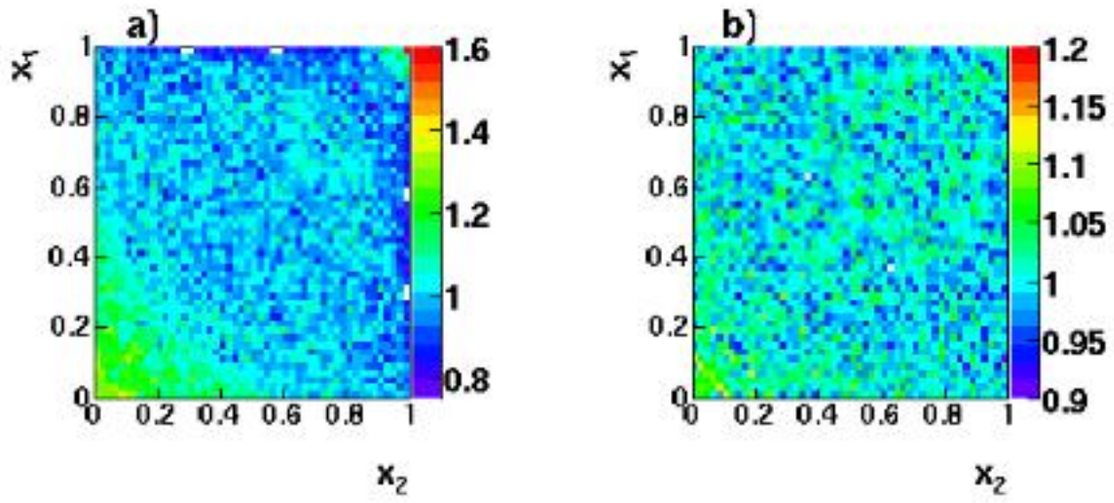


Figure 13

- HIJING model for p+p and C+C interactions
- Dilution effect from the higher number of particle pairs

# 6. Discussion

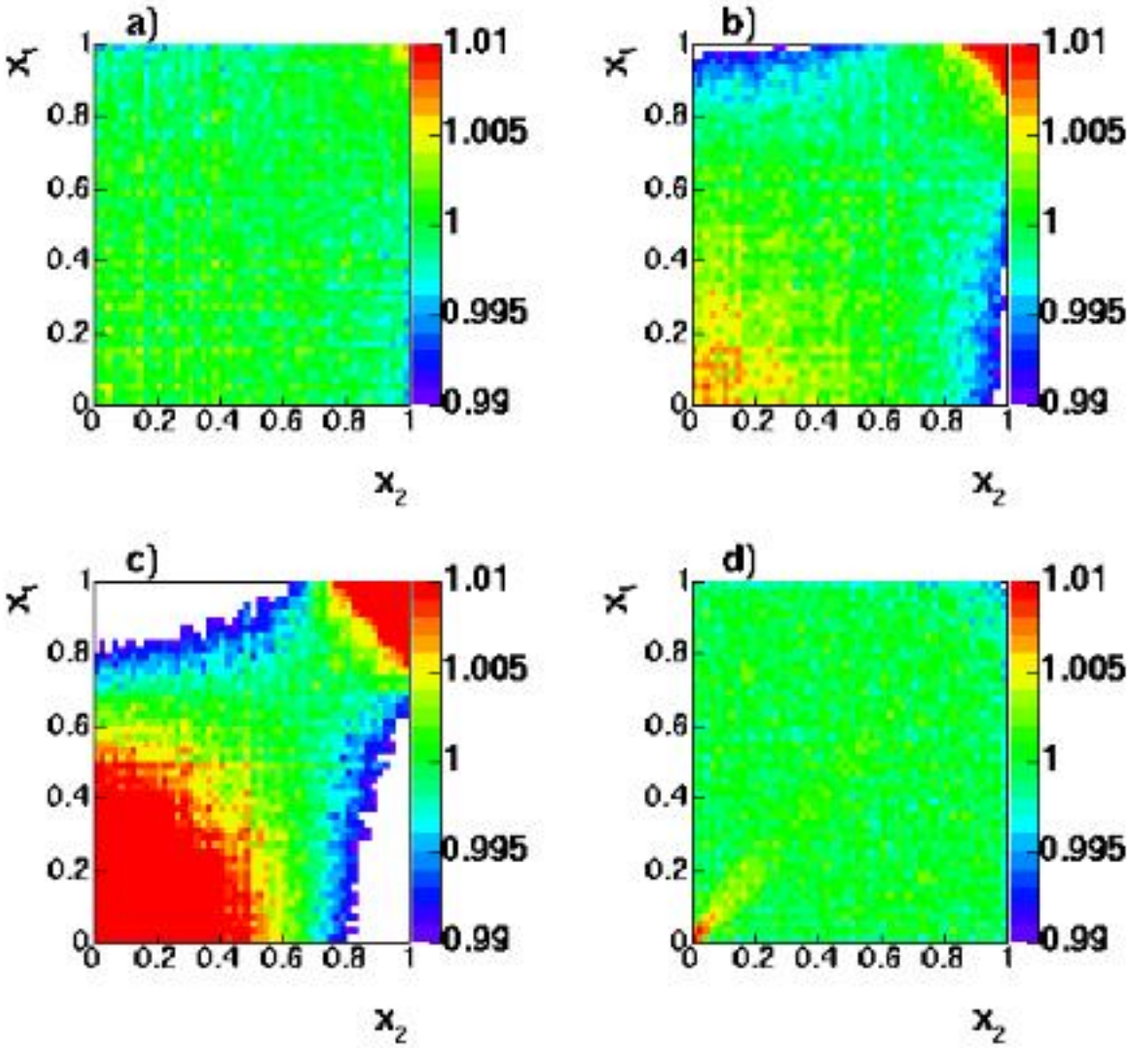


Figure 14

- Model with inverse slope parameter fluctuations for central Pb+Pb
- a) $\sigma(T)/T = 2.6\%$
- b) $\sigma(T)/T = 5.3\%$
- c) $\sigma(T)/T = 10.5\%$
- d) Pb+Pb data

# 6.Discussion

- $\sigma(T)/T < 1\%$

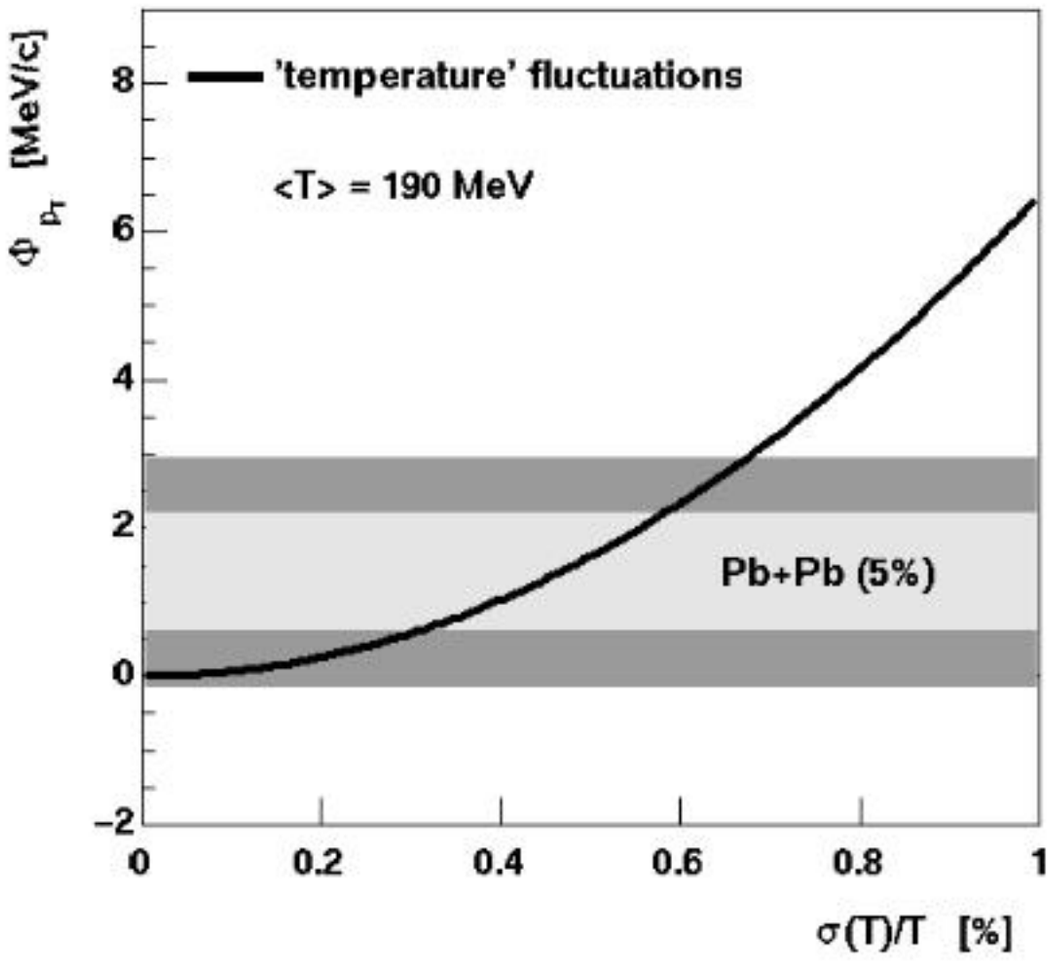


Figure 15

# 6. Discussion

- STAR
- Central Au+Au at sqrt(s) = 130 GeV
- $M(p_T)$ distribution 20% wider than corresponding Gamma distribution
- Saddle shaped structure for two-particle correlation plot
- $\phi_{pT}$ about 25 MeV/c for midrapidity

- PHENIX
- Central Au+Au at sqrt(s) = 130 GeV
- No effect for $M(p_T)$ and $\phi_{pT}$
- The reason: limited azimuthal angle, limited pseudorapidity, lower $p_T$ cut = 0.2 GeV/c

# 6. Discussion

- NA22
- Elementary interactions at 250 AGeV
- $\phi_{pT}$ dependence on the rapidity region
- Confirmation of our low fluctuations for forward hemisphere
- $\phi_{pT}$ for midrapidity above 25 MeV/c

- CERES
- Pb+Au at 158 AGeV
- $\phi_{pT}$ at midrapidity $= 7.8 \pm 0.9$ MeV/c

# 7. Summary

- Event-by-event fluctuations for p+p, C+C, Si+Si and Pb+Pb at 158 AGeV
- FORWARD rapidity region only
- $M(p_T)$, $\phi_{pT}$ and two-particle correlation plots
- Dynamical fluctuations small, system size dependence
- Two-particle correlation plot for p+p data shows a structure connected with $M(p_T)$ versus N correlation
- A small effect of the Bose-Einstein correlations for central Pb+Pb collisions
- HIJING model reproduces two-particle correlation plots but no $\phi_{pT}$ versus centrality dependence